

Detection of spin polarized currents in quantum point contacts via transverse electron focusing

A. Reynoso, Gonzalo Usaj, and C. A. Balseiro

Instituto Balseiro and Centro Atómico Bariloche, Comisión Nacional de Energía Atómica, (8400) San Carlos de Bariloche, Argentina.

(Dated: submitted 10 october 2006)

It has been predicted recently that an electron beam can be polarized when it flows adiabatically through a quantum point contact in a system with spin-orbit interaction. Here, we show that a simple transverse electron focusing setup can be used to detect such polarized current. It uses the amplitude's asymmetry of the spin-split transverse electron focusing peak to extract information about the electron's spin polarization. On the other hand, and depending on the quantum point contact geometry, including this one-body effect can be important when using the focusing setup to study many-body effects in quantum point contacts.

PACS numbers: PACS numbers: 72.25.Dc,73.23.Ad,75.47.Jn,71.71.Ej

I. INTRODUCTION

Important goals in the field of spintronics¹ are the production, detection and manipulation of spin polarized currents in semiconductors. During the last years, there has been several proposals in those directions which go from the use of ferromagnetic materials² to the use of the spin Hall effect in systems with spin-orbit (SO) interaction.^{3,4,5,6,7,8,9,10,11} The latter approach has attracted much of attention due to the non-trivial spin dynamics introduced by the SO coupling.^{12,13,14,15} In a recent work by Eto *et al*¹⁶ a very simple mechanism for creating a spin polarized current was proposed: electrons in a two dimensional gas (2DEG) with SO coupling can be polarized when they pass adiabatically through a constriction that admits only a few conducting channels. Such a constriction could be a quantum point contact (QPC) or simply a potential barrier in a quantum wire—a similar effect was predicted by Silvestrov and Mishchenko.¹⁷ The origin of such polarization, discussed below, is related to the spin structure of the energy sub-bands inside the constriction or barrier. Despite this seemingly simple way to create a spin polarized current, this effect has not been observed yet. One of the reasons is that its detection requires the use of a spin analyzer, which is not a trivial task.

In this work, we show that a two terminal device is not efficient to detect such spin polarized current and propose to use transverse electron focusing to measure it. Transverse focusing experiments are done in a solid state device in which electrons emitted from a QPC are focalized onto a collector (another QPC) by the action of an external magnetic field perpendicular to the 2DEG—in a classical picture, the electrons are forced to follow circular orbits due to the Lorentz force. For values of the external field B_n such that the distance between the QPCs is n times the diameter of the cyclotron orbit, with n an integer number, the electrons enter the collector and create a charge accumulation in it that generates a voltage difference. This gives voltage peaks as the external field is swept through the focusing fields B_n .¹⁸ As shown in Refs. [19,20], in systems with spin-orbit coupling the first focusing peak splits in two. Furthermore, each peak corresponds to a different spin projection of the electron leaving the emitter.¹⁹ If the emitted electrons were unpolarized, both peaks would have the same intensity. Conversely, if the electrons leaving

the emitter are polarized, the intensity of the two peaks must be different. The intensity difference of the two peaks is then a direct measurement of the spin polarization of the current induced by the emitter. This very simple idea was recently used in Ref. [21] to study the current's spin polarization induced by the '0.7' anomaly in a QPC. Our results are also relevant in that context, since they shown that one-body effects can substantially contribute to the peak's height asymmetry. It might then be difficult to distinguish one-body from many-body effects^{22,23,24} using this technique.

II. SPIN POLARIZATION IN A QUANTUM POINT CONTACT

A. The model

We consider a 2DEG with Rashba spin-orbit coupling. The Hamiltonian describing the system is given by

$$H = \frac{p_x^2 + p_y^2}{2m^*} + \frac{\alpha}{\hbar}(p_y\sigma_x - p_x\sigma_y) + V(\mathbf{r}). \quad (1)$$

The first term is the kinetic energy of the 2DEG where m^* is the electron effective mass. The second term describes the Rashba coupling, whose strength is characterized by α , and the last term is the lateral confining potential defined by the external gates. In order to present a quantitative description for arbitrary geometries, the Hamiltonian is integrated numerically using a finite difference scheme—this is equivalent to work with a tight-binding model (see Ref. [25] for details). We first analyze the electronic transport through a barrier or a constriction. The confining potential is $V(\mathbf{r}_n) = V_s(\mathbf{r}_n) + V_c(\mathbf{r}_n)$, where $V_s(\mathbf{r}_n)$ defines the shape of the sample (a hard wall potential) and $V_c(\mathbf{r}_n)$ the structure of the barrier or QPC. In what follows, we use two different models for V_c and analyze their effectiveness to spin-polarize the transport current. The SO coupling α is set to zero at the source and drain reservoirs—described as ideal leads—and it is turned on adiabatically at the lead-sample interface using either a hyperbolic tangent function or a simple linear function to describe its spatial profile (see Fig. 1a).^{25,26,27}

In the linear response regime, the conductance is given by $G = (e^2/h)\text{Tr}[\mathbf{\Gamma}^R \mathbf{G}^r(E_F) \mathbf{\Gamma}^L \mathbf{G}^a(E_F)]$, where $\mathbf{G}^{r(a)}(\epsilon)$ is

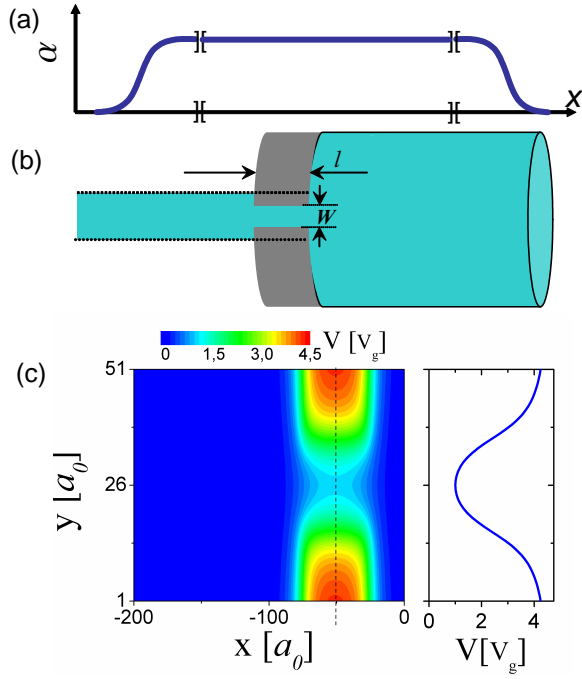


FIG. 1: (color online) (a) Schematic representation of the spatial profile of the SO coupling α . The coupling is turned on and off in 300 lattice sites. (b) Schematics of the system's geometry. The period lead (800 sites wide) at the right of the QPC is introduced to avoid the oscillation of the polarization as a function of the sample-lead interface (see text). (c) potential profile corresponding to Eq. (2)

the retarded (advanced) matrix propagator, with elements $\mathbf{G}_{i\sigma,j\sigma'}^r(\varepsilon)$ given by the propagator from site j and spin σ' to site i and spin σ , $\mathbf{\Gamma}_{i\sigma,j\sigma'}^{L(R)} = i(\mathbf{\Sigma}_{L(R)}^r - \mathbf{\Sigma}_{L(R)}^a)_{i\sigma,j\sigma'}$ where $\mathbf{\Sigma}_{L(R)}^{r(a)}$ is the retarded (advanced) self-energy due to the left (right) contact and E_F is the Fermi energy. The SO coupling acts as an effective magnetic field contained in the plane of the 2DEG with a magnitude that is proportional the momentum of the carrier. This effective field lifts the spin degeneracy of the bands. For the wire geometry it is convenient to quantize the spins along the transverse axis (y -axis). In what follows \uparrow and \downarrow indicate the two spin projections along this direction.

To study the current spin polarization, we calculate the spin-resolved conductance $G_{\sigma'\sigma}$ that describes the contributions due to the electrons that are injected from the left lead with spin σ and collected at the right lead with spin σ' . The polarization P of the transmitted current is then defined as $P = \sum_{\sigma} (G_{\uparrow\sigma} - G_{\downarrow\sigma}) / \sum_{\sigma\sigma'} G_{\sigma'\sigma}$. We first consider the following potential¹⁶

$$V_c(x,y) = \frac{V_g}{2} \left(1 + \cos \frac{\pi x}{L_x}\right) + \frac{\eta E_F}{\Delta^2} \sum_{s=\pm} (y - y_s(x))^2 \theta[s(y - y_s(x))], \quad (2)$$

which is defined for $|x| \leq L_x = L_1 \theta(-x) + L_2 \theta(x)$ and it is zero otherwise. $L_1 + L_2$ is the total length of the potential barrier, $y_{\pm}(x) = \pm(L_y/4)[1 - \cos(\pi x/L_x)]$ gives the shape of the lateral

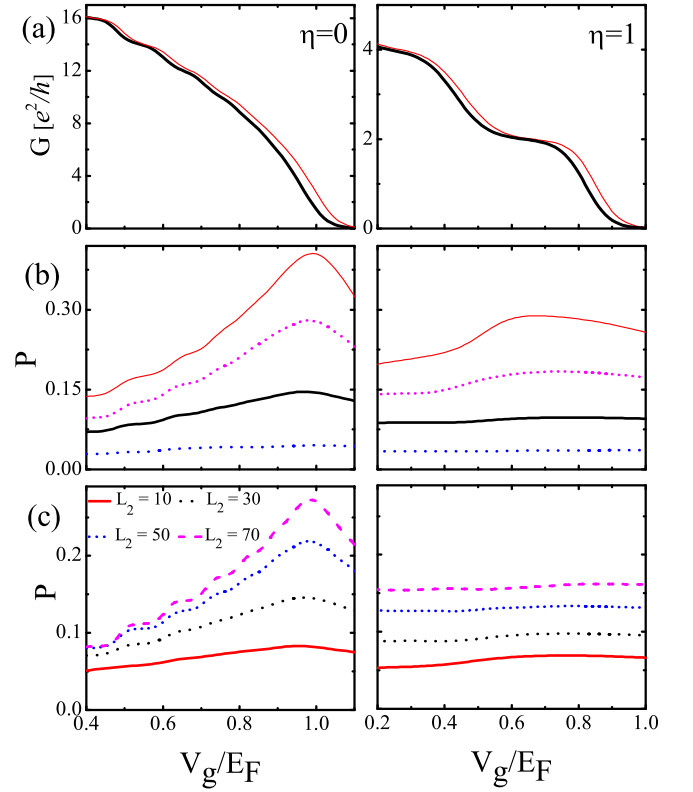


FIG. 2: (color online) Conductance (a) and polarization (b, c) for different geometries ($\eta = 0$, left and $\eta = 1$, right panel) and values of the SO-coupling α as a function of the gate potential V_g . The common parameters are $L_y = 51a_0$, $L_1 = L_2 = 30a_0$, $E_F = 10\text{meV}$, $m^* = 0.067m_0$, $\Delta = L_1/4$ and the lattice parameter $a_0 = 5\text{nm}$. (a) conductance for $\alpha = 5\text{meVnm}$ (thick line) and 20meVnm (thin line); (b) polarization for $\alpha = 5$ (dotted line), 10 (solid line), 15 (shot-dotted line), and 20meVnm (thin solid line); (c) polarization for $\alpha = 10\text{meVnm}$ and different values of L_2 .

constriction, and $\theta(x)$ is the step-function. This model potential has the virtue that the relevant parameters can be easily changed. The gate potential V_g controls the height of the potential barrier at $x=0$ and then the conductance.

Before presenting the results, it is important to emphasize here the role play by the sample-lead interface (the point where α is turned off). We have found that, in narrow wires, the polarization of the current strongly depends on the position of such interface. In fact, the polarization shows an oscillating pattern as a function of the distance between the QPC and the sample-lead interface. The oscillation originates from the scattering of the electrons at the edges of the wires before reaching the sample-lead interface. To avoid this effect, we introduced a large periodic lead at the output of the QPC as shown in Fig. 1b.²⁸

Figure 2 shows the conductance and the polarization as a function of the gate potential V_g for different values of the parameters. Left panels correspond to $\eta = 0$, a simple potential barrier, while the right panels correspond to $\eta = 1$, a QPC. In Fig. 2a the conductance is shown for different values of α ; as it increases the conductance curve is shifted towards a higher

gate potential, as expected. Except for that, the total conductance is not sensitive to the Rashba coupling. Note that for $\eta = 0$ the conductance steps are not well defined. It is worth notice that the latter case is not in the regime where a jump on the conductance at the opening of the barrier is expected.¹⁷ Figure 2b shows the current polarization for $\alpha = 5, 10, 15, 20$ meVnm. The polarization increases with α monotonically. The polarization for $\alpha = 10$ meVnm and different values of L_2 is shown in Fig. 2c. Clearly, P increases with L_2 while it is essentially independent of L_1 (not shown).¹⁶

These results are consistent with the ideas put forward in Ref. [16]. The spin filtering effect arises from the avoided crossings (caused by the term $\frac{\alpha}{\hbar} p_y \sigma_x$ in (1)) between different spin-dependent sub-bands (channels associated to the term $p_x^2/2m^* - \frac{\alpha}{\hbar} p_x \sigma_y$). These avoided crossings generate an adiabatic spin rotation as the electrons leave the QPC, hence the strong dependence on L_2 (the parameter that controls adiabaticity). The picture also explains why the total conductance is not affected, as the number of propagating channels inside the QPC do not change. The partial conductance $G_{\uparrow} = \sum_{\sigma} G_{\uparrow, \sigma}$ and $G_{\downarrow} = \sum_{\sigma} G_{\downarrow, \sigma}$ are, in general, very different from each other. Usually, in the first plateau, G_{\uparrow} is larger than e^2/h , which indicates that for the transmitted electrons with spin \uparrow there is more than one channel that contributes. In particular, one can find cases where $P \simeq 1$, so that $G_{\downarrow} \simeq G_{\uparrow} \simeq G_{\downarrow} \simeq 0$ and $G_{\uparrow} \simeq 2e^2/h$ (see Ref. [26]). In this extreme case, only spin up electrons are transmitted. However, spins rotate as electrons enter and leave the QPC and both spins contribute to the charge current inside the QPC.

The fact that $P \neq 0$ is quite general. It does not depend on the details of the potential $V_c(\mathbf{r})$ as far as adiabaticity is guarantee. We have verified this by computing the conductance and the polarization for different potential profiles. From hereon, we use a more realistic potential corresponding to rectangular gates of length l , separated a distance W from each other and located at a distance z from the 2DEG,²⁹

$$V(x, y) = V_g [f(x_-, y_+) - f(x_+, y_+) + f(x_-, -y_-) - f(x_+, -y_-)] \quad (3)$$

with $x_{\pm} = x/z \pm l/2z$, $y_{\pm} = y/z \pm W/2z$ and

$$f(u, v) = \frac{1}{2\pi} \left[\frac{\pi}{2} - \arctan(u) - \arctan(v) + \arctan \left(\frac{uv}{\sqrt{1+u^2+v^2}} \right) \right] \quad (4)$$

In the following, we use $z = 30\text{nm}$, $l = 250\text{nm}$ and $W = 100\text{nm}$

B. The effect of magnetic fields

We now analyze the effect of both a small out-of-plane magnetic field, which couples to the spin and orbital degrees of freedom, and an in-plane field, which couples to the spins only. As we show below, the polarization P is more sensitive to the presence of an in-plane field.

The presence of an out-of-plane field B_z is described by including a term $H_z = g\mu_B \sigma_z B_z$ and replacing the momentum \mathbf{p}

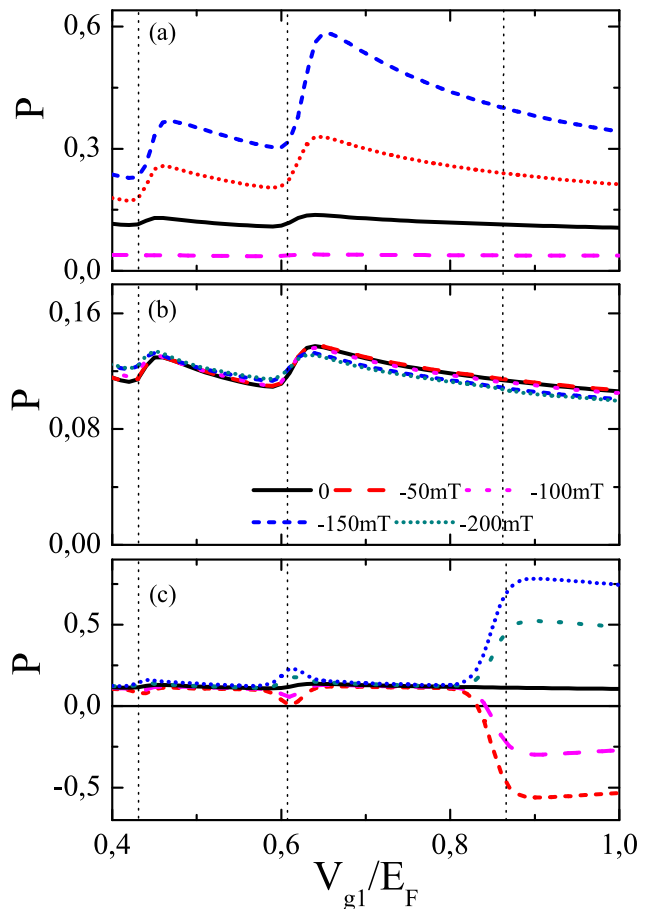


FIG. 3: (color online) Polarization as a function of V_g in a more realistic potential profile (see text). The vertical lines correspond to $G = e^2/h$ and $G = 3e^2/h$. (a) for $\alpha = 5, 10, 15, 20\text{meVnm}$ (dashed, solid, dotted, short-dashed line, respectively). (b) for different values of B_z and $\alpha = 10\text{meVnm}$. (c) for different values of the Zeeman energy $g\mu_B B_{\parallel} = -0.25\text{meV}, -0.125\text{meV}, 0\text{meV}, 0.125\text{meV}, 0.25\text{meV}$ (short-dashed, dashed, solid, dotted and short dotted line, respectively) and α as in (b). Notice that for $B_{\parallel} \neq 0$, the polarization has an abrupt change when the conductance reaches the first plateau and that for $B_{\parallel} < 0$ it can even change sign.

by $(\mathbf{p} + e/c\mathbf{A})$ where \mathbf{A} is the vector potential associated with B_z . In the tight-binding representation, the latter is included as a Peierls substitution.¹⁹ Both the conductance (not shown) and the polarization are relatively insensitive to the presence of B_z in the explored range $[0, 200\text{mT}]$. In the case of the conductance, the field does not generate a splitting of the plateaus but a weak double shoulder. This effect, which is much larger than what it is expected from the Zeeman term, is originated by the diamagnetic coupling.³⁰

The case of an in-plane field along the y -axis is shown in figure 3c. Since the transmitted current is polarized in the y -direction, a field pointing in the same direction tends to increase or decrease the effect depending on its sign. This is clearly seen in the figure, in particular before the first plateau of the conductance is fully developed—the effect is less pronounced at the opening of the second and third channels. In-

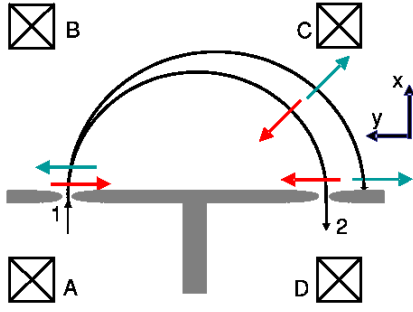


FIG. 4: (color online) Schematic representation of the setup used to detect spin polarization. The focusing signal is the voltage V_{CD} as a function of B_z

terestingly, for the parameters of the figure and a field such that $g\mu_B B_{\parallel} = 0.125\text{meV}$, which for $g = 0.5$ corresponds to $B_{\parallel} \simeq 5\text{T}$, P changes sign for a gate potential V_g corresponding to $G \simeq e^2/h$. This shows that the interplay between SO coupling and an external in-plane field could be used to select the desired polarization of the current transmitted through a QPC.

III. DETECTION USING TRANSVERSE ELECTRON FOCUSING

Even in the presence of external fields, a direct measurement of transport properties in two terminal devices does not provide any evidence of the spin polarization of the transmitted current. We have verified that neither the shot noise nor the thermopower show any significant feature even in the case of large P . To measure P it is then necessary to design an experiment with a more complex geometry. In the following, we discuss how transverse electron focusing can give a direct measurement of the polarization induced by the QPC.

The transverse electron focusing setup is shown in Fig. 4: a current I_{AB} is injected through the first QPC while the voltage drop V_{CD} is measured in the second QPC.³¹ V_{CD} shows then a series of peaks every time $R/2r_c$ is an integer number. Here, R is the distance between the QPCs (of the order of $1\mu\text{m}$) and r_c is the cyclotron radius. For the purpose of the present work we can assume³² that $V_{CD} \propto T_{AD}$, where T_{AD} is the transmission probability from one QPC to the other. In the presence of SO coupling, the first focusing peak is split in two, each peak corresponding to a different spin orientation of the electrons leaving the emitting QPC.^{19,20,33,34,35}

Figure 5a shows typical results for T_{AD} as a function of B_z for different values of V_{g1} and B_{\parallel} . Clearly, the asymmetry of the peaks height results from the polarization of the electrons as they are transmitted through the first QPC. Therefore, such difference is a measure of P . Figure 5b shows the peak's height difference (normalized to the sum) as a function of V_{g1} for $\alpha = 10\text{meVnm}$ and $g\mu_B B_{\parallel} = 0, 0.25\text{meV}$ and -0.25meV . This clearly reveals the presence of a spin polarized current and allows to quantify it. A close comparison

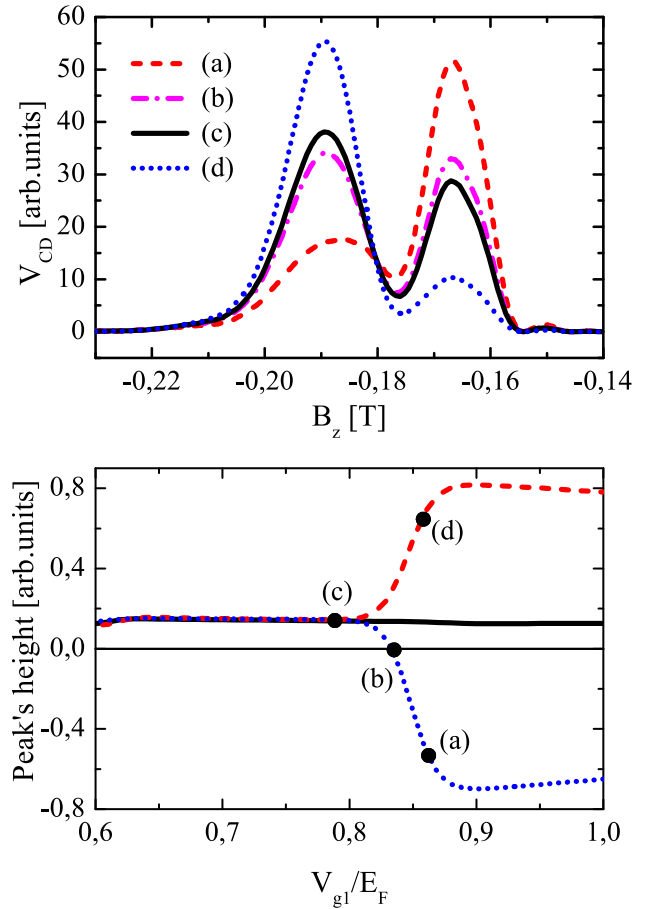


FIG. 5: (color online) Top: Spin-split first focusing peak for different values of V_{g1} and B_{\parallel} as indicated. Peaks are normalized to have the same area. Notice the contrast in the peaks' magnitude, reflecting the different values of polarization of the electrons emitted by the QPC. Bottom: Polarization, as extracted from the peaks' height, as a function of V_{g1} for $\alpha = 10\text{meVnm}$ and $g\mu_B B_{\parallel} = 0, 0.25\text{meV}$ and -0.25meV (solid, dashed and dotted lines, respectively). These results compare nicely with those of Fig. 3c and shown that information about P can be extracted from the focusing signal.

with Fig. 3c, however, show some quantitative differences. The main difference comes from the fact that in the focusing geometry both QPCs lead to some spin polarization. A simple estimate for the 'measured' polarization P_m is given by $P_m = (P_1 - D)/(1 - P_1 D)$ where P_1 is the spin polarization introduced by the first QPC and $D = \sum_{\sigma} (G_{\sigma\uparrow} - G_{\sigma\downarrow}) / \sum_{\sigma\sigma'} G_{\sigma'\sigma}$ is a filtering factor that measure the transmission difference of the two spin projections through the second QPC (for a symmetric QPC, $D = -P$). We checked this relation by turning on and off the SO coupling in the second QPC. Experimentally, this could be avoided by using a different geometry for the second QPC (less adiabatic) so that $D \ll 1$ and then $P_m \simeq P_1$.

It is important to emphasize that the behavior of P as a function of V_{g1} in the region where the QPC starts conducting is, in general, the opposite to the one observed in a sample with a two dimensional hole gas, see Ref. [21]. That is, the polarization increases as the QPC opens up—there are some ex-

amples of a decrease of the polarization (see Fig. 2) though the changes of P is rather small. This increase of P is also expected based on the theoretical arguments explained above for either Rashba or Dresselhaus SO coupling.

IV. SUMMARY

We showed that the spin polarized current generated by a QPC in systems with Rashba spin-orbit coupling can be measured using a transverse electron focusing setup. This is possible because the difference in amplitude of the spin-split focusing peaks is proportional to the spin polarization of the electrons leaving the emitting QPC.

In addition, we also showed that the interplay between SO coupling and an in-plane magnetic field could be used to independently select the desired sign of the polarization of the current transmitted through a given QPC. This is quite different for the case without SO,¹⁸ where only the magnitude of the polarization can be changed and where the sign of the polarization would be the same in all the QPCs present on the

system.

Finally, we found that current polarization increases with the conductance of the QPC as it goes from zero to $2e^2/h$. As mentioned above, this is just the opposite behavior that was observed in Ref. [21]. It is not clear to us at this point what is the origin of this discrepancy. One possibility is the different nature of the spin-orbit coupling in electron and hole gases. The other is the presence of many-body effects, which are not included in our calculation. In the latter case, the temperature dependence of the observed polarization might provide a way to distinguish between both contributions as we expect the one-body SO effect described here to be rather insensitive to temperature as far as kT is smaller than $2\alpha k_F$. This is a very interesting point that deserves further investigation.

V. ACKNOWLEDGEMENT

This work was supported by ANPCyT Grants No 13829 and 13476 and CONICET PIP 5254. AR and GU acknowledge support from CONICET.

-
- ¹ D. Awschalom, N. Samarth, and D. Loss, eds., *Semiconductor Spintronics and Quantum Computation* (Springer, New York, 2002).
 - ² S. Datta and B. Das, *Appl. Phys. Lett.* **56**, 665 (1990).
 - ³ M. I. Dyakonov and V. I. Perel, *JETP Lett.* **13**, 467 (1971), *Phys. Lett. A* **35**, 459 (1971).
 - ⁴ J. E. Hirsch, *Phys. Rev. Lett.* **83**, 1834 (1999).
 - ⁵ J. C. Egues, G. Burkard, and D. Loss, *Applied Physics Letters* **82**, 2658 (2003).
 - ⁶ S. Murakami, N. Nagaosa, and S. C. Zhang, *Science* **301**, 1348 (2003).
 - ⁷ J. Sinova, D. Culcer, Q. Niu, N. A. Sinitsyn, T. Jungwirth, and A. H. MacDonald, *Phys. Rev. Lett.* **92**, 126603 (2004).
 - ⁸ L. W. Molenkamp, G. Schmidt, and G. E. W. Bauer, *Phys. Rev. B* **64**, 121202 (2001).
 - ⁹ V. Sih, R. C. Myers, Y. K. Kato, W. H. Lau, A. C. Gossard, and D. D. Awschalom, *Nature* p. 31 (2005).
 - ¹⁰ H.-A. Engel, B. I. Halperin, and E. I. Rashba, *Phys. Rev. Lett.* **95**, 166605 (2005).
 - ¹¹ V. Sih, W. H. Lau, R. C. Myers, V. R. Horowitz, A. C. Gossard, and D. D. Awschalom, *Phys. Rev. Lett.* **97**, 096605 (2006).
 - ¹² E. G. Mishchenko and B. I. Halperin, *Phys. Rev. B* **68**, 045317 (2003).
 - ¹³ J. Schliemann and D. Loss, *Phys. Rev. B* **68**, 165311 (2003).
 - ¹⁴ J. Schliemann, D. Loss, and R. M. Westervelt, *Physical Review Letters* **94**, 206801 (2005).
 - ¹⁵ B. K. Nikolic, L. P. Zarbo, and S. Welack, *Phys. Rev. B* **72**, 075335 (2005).
 - ¹⁶ M. Eto, T. Hayashi, and Y. Kurotani, *J. Phys. Soc. Jpn.* **74**, 1934 (2005).
 - ¹⁷ P. G. Silvestrov and E. G. Mishchenko, *Phys. Rev. B* **74**, 165301 (2006).
 - ¹⁸ R. M. Potok, J. A. Folk, C. M. Marcus, and V. Umansky, *Phys. Rev. Lett.* **89**, 266602 (2002).
 - ¹⁹ G. Usaj and C. A. Balseiro, *Phys. Rev. B* **70**, 041301(R) (2004).
 - ²⁰ L. P. Rokhinson, V. Larkina, Y. B. Lyanda-Geller, L. N. Pfeiffer, and K. W. West, *Phys. Rev. Lett.* **93**, 146601 (2004).
 - ²¹ L. P. Rokhinson, L. N. Pfeiffer, and K. W. West, *Phys. Rev. Lett.* **96**, 156602 (2006).
 - ²² T. Rejec and Y. Meir, *Nature* **442**, 900 (2006).
 - ²³ M. Kindermann, P. W. Brouwer, and A. J. Millis, *Phys. Rev. Lett.* **97**, 036809 (2006).
 - ²⁴ P. Cornaglia and C. Balseiro, *Europhys. Lett.* **67**, 634 (2004).
 - ²⁵ A. Reynoso, G. Usaj, and C. A. Balseiro, *Phys. Rev. B* **73**, 115342 (2006).
 - ²⁶ A. Reynoso, G. Usaj, and C. A. Balseiro, *Physica B* **384**, 28 (2006).
 - ²⁷ The case of a coordinate dependent SO-coupling requires a proper symmetrization of the Rashba term.
 - ²⁸ In this geometry, there is still a small decaying oscillation around the mean value which arises from the the multiple reflexion between the sample-lead interface and the hard wall potential that describes the QPC far from its center. In this case the oscillation have a well defined wavelength, $\lambda = \pi\hbar^2/m^*\alpha$ so it can be easily averaged out.
 - ²⁹ D. K. Ferry and S. M. Goodnick, *Transport in Nanostructures* (Cambridge University Press, New York, 1997), p. 180.
 - ³⁰ S. Debal and B. Kramer, *Phys. Rev. B* **71**, 115322 (2005).
 - ³¹ H. van Houten, C. W. J. Beenakker, J. G. Williamson, M. E. I. Broekaart, P. H. M. Loosdrecht, B. J. van Wees, J. E. Mooji, C. T. Foxon, and J. J. Harris, *Phys. Rev. B* **39**, 8556 (1989).
 - ³² C. W. Beenakker and H. van Houten, in *Solid State Physics*, edited by H. Ehrenreich and D. Turnbull (Academic Press, Boston, 1991), vol. 44, pp. 1–228.
 - ³³ A. Reynoso, G. Usaj, M. J. Sanchez, and C. A. Balseiro, *Phys. Rev. B* **70**, 235344 (2004).
 - ³⁴ J. J. Heremans, reported at ICPS 28, Vienna (2006).
 - ³⁵ A. Dedigama, D. Deen, S. Murphy, N. Goel, J. Keay, M. Santos, K. Suzuki, S. Miyashita, and Y. Hirayama, *Physica E* (2006).